JOURNAL OF AEROSOL MEDICINE AND PULMONARY DRUG DELIVERY
Volume 24, Number ■, 2011

Pp. 1–10
DOI: 10.1089/jamp.2010.0871

An *In Vitro* Assessment of Aerosol Delivery Through Patient Breathing Circuits Used with Medical Air or a Helium–Oxygen Mixture

Andrew R. Martin, Ph.D.,[1] Angela Ang,[1] Ira M. Katz, Ph.D.,[1,2] Sabine Häussermann, Ph.D.,[1,*]
Georges Caillibotte, Ph.D.,[1] and Joëlle Texereau, M.D., Ph.D.[1]

Abstract

Background: The bench experiments presented herein were conducted in order to investigate the influence of carrier gas, either medical air or a helium–oxygen mixture (78% He, 22% O_2), on the droplet size distribution and aerosol mass delivered from a vibrating mesh nebulizer through a patient breathing circuit.
Methods: Droplet size distributions at the exit of the nebulizer T-piece and at the patient end of the breathing circuit were determined by laser diffraction. Additional experiments were performed to determine the effects on measured size distributions of gas humidity and of the droplet residence time during transport from the nebulizer to the laser diffraction measurement volume. Aerosol deposition in the nebulizer, breathing circuit, and on expiratory and patient filters was determined by photometry following nebulization of sodium fluoride solutions into the breathing circuit during simulated patient breathing.
Results: With no humidification of the carrier gas, droplet volume median diameter (VMD) at the exit of the nebulizer T-piece was 5.5 ± 0.1 μm for medical air, and 4.3 ± 0.1 μm for helium–oxygen. Varying the aerosol residence time between the nebulizer and the measurement volume did not affect the measured size distributions; however, humidification of the carrier gases reduced differences in VMD at the nebulizer exit between medical air and helium–oxygen. At the patient end of the breathing circuit, droplet VMDs were 1.8 ± 0.1 μm for medical air and 2.2 ± 0.1 μm for helium–oxygen. The percentages of sodium fluoride recovered from the nebulizer, breathing circuit, patient filter, and expiratory filter were, respectively, 29.9 ± 8.3, 40.4 ± 5.6, 8.3 ± 1.5, and 21.5 ± 2.1 % for air, and 32.6 ± 2.2, 36.3 ± 0.7, 12.0 ± 1.4, and 19.1 ± 1.1 % for helium–oxygen.
Conclusions: Ventilation with helium–oxygen in place of air–oxygen mixtures can influence both the droplet size distribution and mass of nebulized aerosol delivered through patient breathing circuits. Assessment of these effects on aerosol delivery is important when incorporating helium–oxygen into patient ventilation strategies.

Key words: helium–oxygen, nebulizer, droplet size distribution, laser diffraction, aerosol deposition, noninvasive ventilation

Introduction

Recent clinical studies have investigated gas mixtures of helium and oxygen (He/O_2) in combination with noninvasive ventilation (NIV) to treat acute exacerbations of chronic obstructive lung disease (COPD).[1,2] Briefly, for patients with obstructive lung disease, the beneficial effects of breathing He/O_2 stem from the low density of the mixture, which is approximately one-third that of air. Density-dependent components of airway resistance, including those arising from both turbulence and convective acceleration of gas flow through the tracheobronchial airways, are reduced when breathing He/O_2 in place of air or air/O_2 mixtures.[3,4] Accordingly, combining He/O_2 with positive pressure support during NIV reduces patient effort[3] and dyspnea[5] during acute exacerbations of COPD.

[1]Medical Gases Group, Air Liquide Santé International, Centre de Recherche Claude-Delorme, Jouy-en-Josas, France.
[2]Department of Mechanical Engineering, Lafayette College, Easton, Pennsylvania.
*Current address: Inamed GmbH, Gauting, Germany.

Delivery of aerosolized bronchodilators is standard in treating exacerbations of COPD,[6,7] whereas aerosol delivery of corticosteroid[8,9] and combination corticosteroid/bronchodilator[10] therapies has been explored. For patients receiving NIV, aerosol therapy may be delivered in-line into the ventilator circuit, or during breaks between periods of ventilator support, depending on the practices of the institution administering care.[11,12] Although He/O_2 has previously been shown to influence aerosol delivery through a conventional mechanical ventilation breathing circuit,[13] these results are specific to the delivery devices and breathing circuit studied. As such, the influence of He/O_2 on aerosol delivery during NIV should be evaluated for a given combination of delivery device and breathing circuit prior to employing that combination for coadministration of He/O_2 and aerosol therapy. Further, as He/O_2 is known to affect droplet size distributions delivered from jet nebulizers,[14–17] and, though less so, from vibrating mesh nebulizers,[16,18] these modalities of aerosol delivery may require particular attention.

The experiments described below were conducted in order to investigate the effects of He/O_2 in place of air on aerosol delivery from Aeroneb Solo vibrating mesh nebulizers through the breathing circuit of a Hamilton G5 ventilator, ahead of employing this combination in a clinical study. The ventilator includes an optional He/O_2 module, which allows accurate control and monitoring of delivered flows, volumes, and gas concentrations when ventilating with He/O_2 mixtures. The availability of appropriate and well-characterized delivery devices is an important step towards wider integration of He/O_2 into clinical practice.[19,20] In the present work, the influence of He/O_2 on both the size of droplets and the aerosol mass delivered through the breathing circuit was evaluated.

Materials and Methods

Gases

All experiments were performed using mixtures of helium and oxygen (78% He, 22% O_2 by volume) or medical air (78% N_2, 22% O_2 by volume). The temperature and water vapor content of the mixtures was measured using a temperature–humidity probe (HC2-C05; Rotronic SARL, France). As supplied, the gas mixtures were at room temperature of $25 \pm 2^{\circ}C$ and contained 0% relative humidity (RH).

Laser diffraction measurement apparatus

Droplet size distributions were measured by laser diffraction (Helos/BF with Inhaler dispersion module; Sympatec GmbH, Germany). A detailed review of laser diffractometry as it relates to sizing of medical aerosols can be found in Mitchell et al.,[21] whereas more recent publications explore the technique for sizing droplets produced by vibrating mesh nebulizers in particular.[18,22]

The apparatus used to supply nebulized aerosol to the laser diffraction system is depicted in Figure 1. The total flow through the measurement region was determined through a vacuum control valve adjusted according to the differential pressure across a venturi tube. This total flow consisted primarily of He/O_2 or air supplied through a mass flow controller (El-Flow Select; Bronkhorst High Tech, Holland)

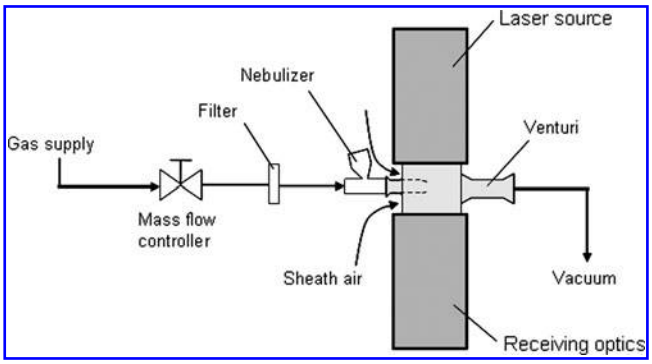

FIG. 1. Schematic of the laser diffraction measurement apparatus.

calibrated for either gas, but also included a smaller fraction of sheath air drawn from the room. This sheath flow helped to prevent deposition of droplets on the windows of the measurement chamber. As shown schematically in Figure 1, the sheath air entered the measurement chamber through two open screw-type valves, but was kept from mixing with the aerosol stream prior to the measurement through the use of a custom designed inlet (Activaero GmbH, Germany) that extended into the chamber just up to the point of intersection with the laser beam, as described previously.[18]

For air, the difference between the vacuum flow rate and the supplied gas flow rate determined the sheath air flow rate. For He/O_2, however, the influence of gas density on the flow-pressure drop relationship of the venturi tube created a complication. Not only did the venturi have to be calibrated specifically for He/O_2 78/22, but also a correction for the dilution of He/O_2 with sheath air was required. Figure 2 displays venturi calibration data for both medical air and He/O_2. To take these measurements, the venturi tube was disconnected from the laser diffraction system, and a series of known flow rates of air or He/O_2 was supplied through a long, straight tube to the venturi. The pressure drop across the venturi tube was measured using a digital manometer (Model PR205; Eurolec Instrumentation Ltd., Ireland).

Also indicated in Figure 2 are predicted values for He/O_2 made by applying the following correction to the air data:

$$Q_{He/O_2} = \sqrt{\frac{\rho_{air}}{\rho_{He/O_2}}} Q_{air} \quad (1)$$

wherein Q_{air} and $Q_{He/O2}$ are volume flow rates for air and He/O_2, respectively, while ρ_{air} and $\rho_{He/O2}$ represent the gas densities.

The correction provided by Equation (1) assumes that all pressure losses in the venturi tube were inertial, that is, that viscous losses were negligible. The very close agreement between measured and predicted values for He/O_2 in Figure 2 indicates that this assumption was appropriate. Accordingly, for a mixture of He/O_2 with sheath air, the mixture flow rate can be determined from the pressure drop across the venturi by correcting the calibration for air as follows:

$$Q_{mix} = \sqrt{\frac{\rho_{air}}{\rho_{mix}}} Q_{air} \quad (2)$$

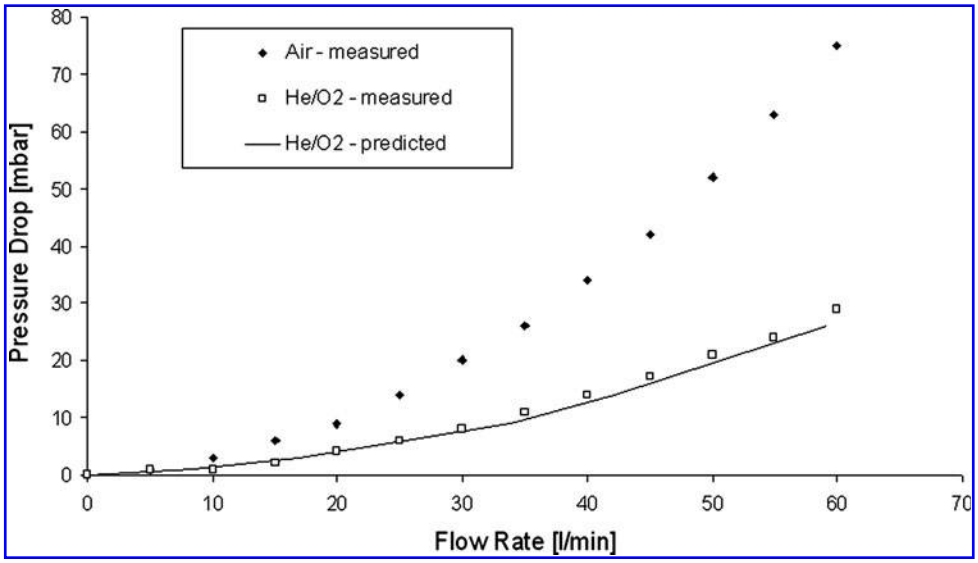

FIG. 2. The pressure drop across the venturi tube plotted against the flow rate of air or He/O_2 supplied through the tube. Also shown are predicted values for He/O_2 made by applying a density-based correction factor [Equation (1)] to the air data.

where

$$Q_{mix} = Q_{He/O_2} + Q_{sheath} \tag{3}$$

and

$$\rho_{mix} = \rho_{air}\frac{Q_{sheath}}{Q_{mix}} + \rho_{He/O_2}\frac{Q_{He/O_2}}{Q_{mix}} \tag{4}$$

For a given pressure drop across the venturi, with Q_{air} calculated from the calibration to air, there then exists a solution to Equations (2)–(4) that allows determination of the amount of sheath air added to a supplied flow of He/O_2. As such, for a fixed supply flow of He/O_2, the sheath flow of room air could be adjusted using the vacuum control valve while observing the pressure drop across the venturi. After preliminary experiments to investigate the influence of the sheath air flow rate on measured droplet sizes, all subsequent measurements were conducted with a supplied gas flow rate of 20 L/min and a sheath air flow rate of 5 L/min. For these flows, the optical concentration, which indicates the amount of light obscuration between the laser source and photo detectors of the laser diffraction apparatus, was within 1–20% for all experimental conditions studied.

Droplet size measurements

All measurements were made on droplets emitted from Aeroneb Solo (Aerogen Ltd., Ireland) nebulizers initially filled with 2 mL of isotonic saline. Nebulization was allowed to continue until completion, and droplets sizes were averaged over 10-sec intervals at the start of each minute of nebulization. For each set of experimental conditions, three separate nebulizations were performed ($n = 3$). Droplet-size distributions were determined from scattering patterns through application of Lorentz–Mie optical theory, using a complex refractive index of $1.33 + 0i$ for the droplet phase. Mean volume median diameters (VMDs) and geometric standard deviations (GSDs) are reported below, the latter calculated as the square root of the d_{84}/d_{16} ratio, where d_n is defined such that n % of the total aerosol volume is contained in droplets with diameters smaller than d_n.

In initial experiments, the nebulizer T-piece was connected directly to the inlet of the laser diffraction measurement chamber. As a result, the distance between the nebulizer and the point of measurement was 9.3 cm, which corresponded to an average residence time between nebulization and measurement of approximately 80 msec. For this configuration, droplet size distributions were measured in flows of dry air and He/O_2. These measurements were repeated for both air and He/O_2 with the supplied gases conditioned to $30 \pm 2^{\circ}C$ and $60 \pm 3\%$ RH using a respiratory heater/humidifier (MR290; Fisher & Paykel Healthcare Limited, New Zealand) placed in-line, upstream from the nebulizer.

In order to further assess the influence of hygroscopic effects on measured droplet size distributions, different lengths of tygon tubing (19 mm inner diameter) were placed between the nebulizer T-piece and the entrance of the laser diffraction measurement chamber. Experiments were then repeated for dry air and He/O_2 with distances of 15.1 and 24.5 cm between the nebulizer and the point of measurement, corresponding to average residence times of approximately 130 and 210 msec between droplet production and sizing.

Finally, in order to estimate the size of droplets delivered to patient facemasks during NIV, the Aeroneb Solo was inserted into the inspiratory limb of the breathing circuit supplied with the Hamilton G5 ventilator (Hamilton Medical AG, Switzerland). Figure 3 displays the various components of the breathing circuit. During the size measurements, the facemask was disconnected and the elbow tubing was connected directly to the laser diffraction measurement chamber. The expiratory tubing was replaced with a plug, and a steady flow of 20 L/min of dry air or He/O_2 was supplied through the inspiratory tubing, with the sheath flow again held at 5 L/min. As for all prior experiments, droplets sizes were averaged over 10-sec sampling intervals at the start of each minute of nebulization, and nebulization was continued

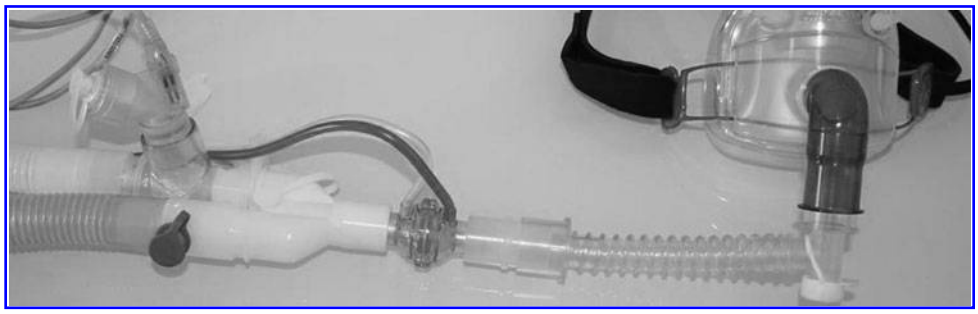

FIG. 3. The breathing circuit, including, from left to right, the nebulizer in the inspiratory arm of the breathing circuit, the Y-piece, the proximal flow sensor, the elbow tubing, and the patient facemask.

until completion. Experiments were repeated in triplicate ($n = 3$).

Aerosol deposition measurements

For deposition measurements, the patient breathing circuit pictured in Figure 3 was used, save that breathing filters (Clearguard II; Intersurgical Inc., UK) were placed between the Y-piece and the expiratory tubing (the expiratory filter), and distal to the elbow tubing (the patient filter). The facemask was removed, and the breathing circuit was connected to one compartment of a dual adult test lung (Michigan Instruments Inc., Grand Rapids, MI, USA). The test lung was ventilated with either dry air or He/O_2 using the Hamilton G5 ventilator in volume control mode. To be consistent with typical breathing patterns measured for pressure support NIV with air/oxygen or He/O_2 during acute exacerbations of COPD,[3,23] ventilation was performed with a tidal volume of 500 mL, 20 breaths per minute, and a ratio between inspiratory time and total breath duration (T_i/T_{tot}) of 0.3.

To measure aerosol deposition in the various components of the breathing circuit, sodium fluoride (NaF) was used as a tracer. A solution containing 6 mg/ml NaF (97%; Acros Organics, Belgium) in distilled water was prepared. This concentration of NaF was chosen to produce a solution with the same osmolarity as isotonic saline, so that droplet vapor pressures and corresponding hygroscopic effects would be similar for the two solutions. The stock solution was diluted to produce a series of standard solutions containing 1.1, 2.2, 4.5, 8.9, and 17.8 μg F^-/mL for use during colorimetric assays (HI 93739; Hanna Instruments Inc., Ann Arbor, MI, USA) similar to those previously described by Waldrep et al.[24] For each experiment, 2 mL of 6 mg/mL NaF solution was nebulized into the inspiratory limb of the breathing circuit during ventilation. After nebulization was complete, ventilation was stopped, and the various components of the breathing circuit were separated and placed in 250 mL crystallization dishes. The nebulizer (including T-piece), Y-piece, flow sensor, elbow tubing, patient filter, and expiratory filter were each washed with known volumes of distilled water to recover deposited NaF. These extract solutions were then diluted into the range of the fluoride photometer for measurement in comparison to the series of standard solutions. Second extracts were performed for the filters and the nebulizer. For the other components, second extracts taken on initial experiments recovered negligible fractions of NaF. From the measured fluoride concentrations and the known extract volumes and dilution ratios, the mass of NaF deposited in each component of the breathing circuit was determined. Experiments were repeated in triplicate for air and He/O_2.

Statistical analysis

For each combination of experimental conditions in which droplet sizes were measured, VMDs in air were compared to those in He/O_2 using a two-tailed Student's *t*-test for independent samples. Likewise, the fractions of NaF recovered from the various components of the breathing circuit were compared between air and He/O_2 using a two-tailed Student's *t*-test for independent samples.

Results

Droplet size measurements

For each experiment, droplets sizes were sampled over 10-sec intervals at the start of every minute of nebulization, so that any changes to the size distribution over the course of nebulization could be observed. However, as the measured size distributions varied little during a single nebulization, droplet sizes were averaged over several time points for every experiment. As each experiment was repeated in triplicate, the droplet size distributions presented below are average distributions both in time and over three experimental repetitions.

Preliminary experiments were performed to assess the influence of the sheath air flow rate through the laser diffraction chamber on measured size distributions. As an example, Figure 4 displays cumulative, normalized, volume-weighted size distributions for droplets nebulized into dry He/O_2 with the sheath flow rate set at either 2 or 5 L/min. Clearly, variation in the sheath air flow rate within this range had little effect on measured size distributions. Similar results were obtained for droplets nebulized into dry air; therefore, as mentioned above, the sheath flow rate was fixed at 5 L/min for all subsequent experiments.

Droplet size distributions produced by the nebulizer supplied with dry air or He/O_2 are compared in Figure 5 for the case where the nebulizer T-piece was connected directly to the inlet of the laser diffraction measurement chamber. Droplet sizes were consistently smaller in He/O_2 than air.

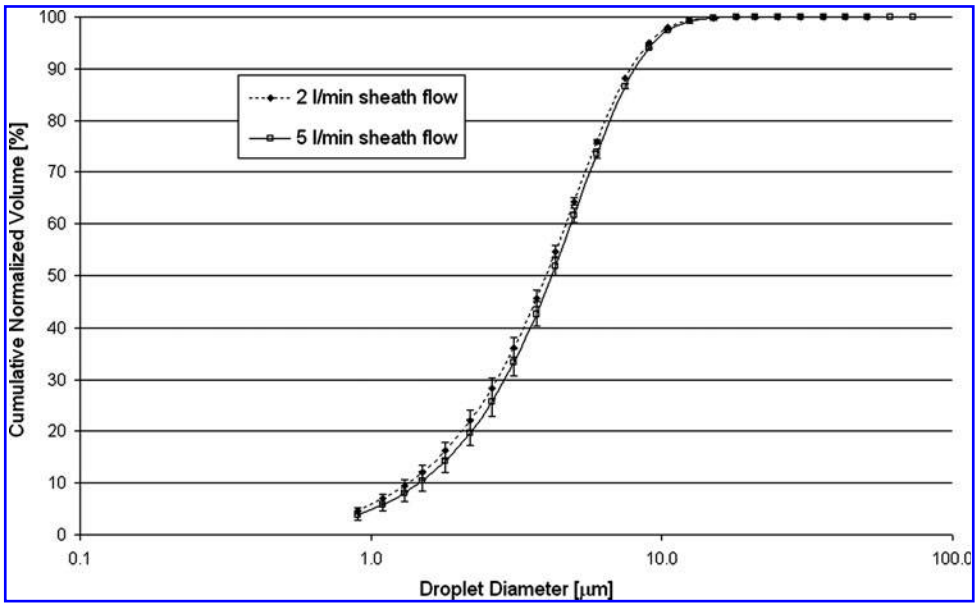

FIG. 4. Droplet size distributions measured for the Aeroneb Solo supplied with 20 L/min of dry He/O_2, using sheath air flow rates of 2 or 5 L/min. Data points are the average of three experiments, and error bars represent 1 standard deviation.

The average size distribution measured in air had a VMD of $5.5 \pm 0.1\ \mu$m (mean $\pm$ 1 standard deviation; $n = 3$) and GSD of 1.77 ± 0.01, while that in He/O_2 had VMD $= 4.3 \pm 0.1\ \mu$m and GSD $= 1.86 \pm 0.004$. This decrease in VMD between air and He/O_2 was statistically significant ($p < 0.001$). Figure 6 displays similar data, but for the case in which the supplied gases were heated and humidified. In this case, the average size distribution measured in air had VMD $= 5.1 \pm 0.1\ \mu$m and GSD $= 1.97 \pm 0.03$, whereas that in He/O_2 had VMD $= 4.5 \pm 0.1\ \mu$m and GSD $= 1.88 \pm 0.03$. Again, size differences between the two carrier gases were statistically significant ($p < 0.01$).

Varying the residence time of droplets between the nebulizer and laser diffraction measurement volume had negligible effect on measured size distributions. This was true for both dry air and He/O_2, as is summarized in Figure 7. In contrast, droplet sizes measured with components of the breathing circuit inserted between the nebulizer and measurement chamber were much smaller than those initially produced by the nebulizer. The average size distribution

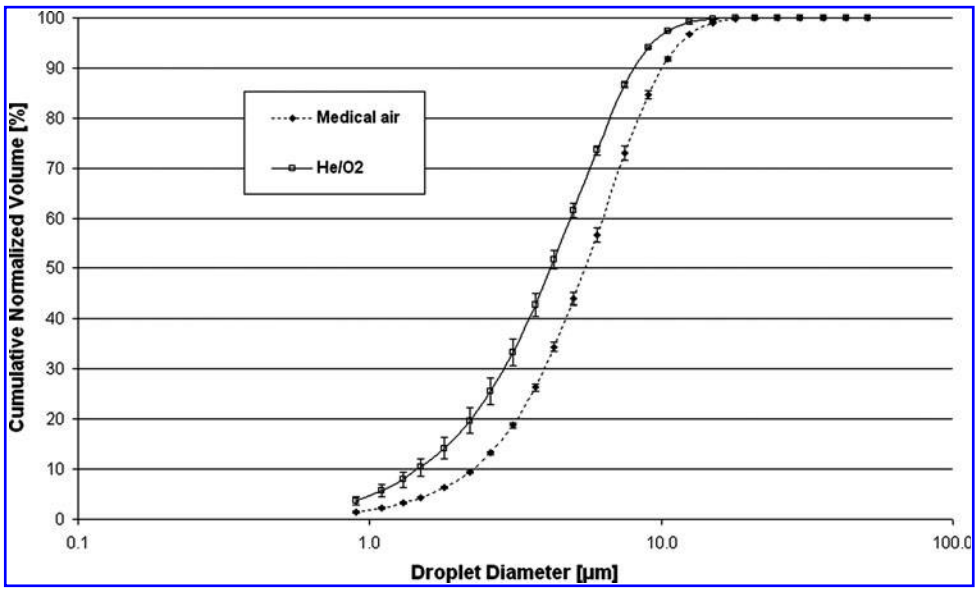

FIG. 5. Droplet size distributions measured with the Aeroneb Solo T-piece connected directly to the inlet of the laser diffraction measurement chamber, with a supply flow of 20 L/min air or He/O_2 at $25 \pm 2^{\circ}$C and 0% RH, and a sheath air flow of 5 L/min. Data points are the average of three experiments, and error bars represent 1 standard deviation.

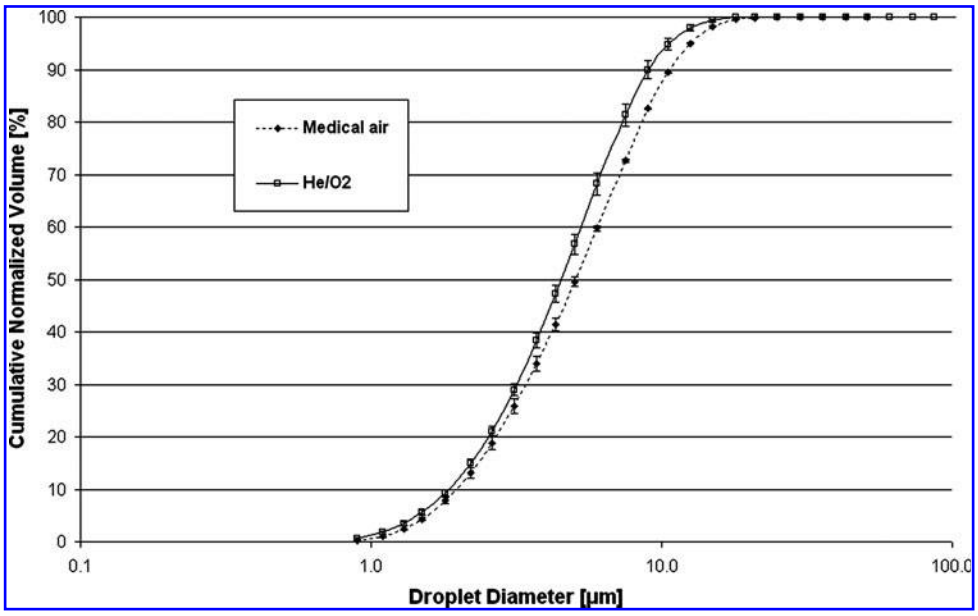

FIG. 6. Droplet size distributions measured with the Aeroneb Solo T-piece connected directly to the inlet of the laser diffraction measurement chamber, with a supply flow of 20 L/min air or He/O_2 at $30 \pm 2^{\circ}C$ and $60 \pm 3\%$ RH, and a sheath air flow of 5 L/min. Data points are the average of three experiments, and error bars represent 1 standard deviation.

measured in air had VMD $= 1.8 \pm 0.1\,\mu$m and GSD $= 2.2 \pm 0.1$, whereas that in He/O_2 had VMD $= 2.2 \pm 0.1\,\mu$m and GSD $= 1.97 \pm 0.03$. The difference in VMD between air and He/O_2 was statistically significant ($p < 0.01$).

Aerosol deposition measurements

Figure 8 displays the mass of NaF, expressed as a percentage of total mass recovery, deposited in the nebulizer (including T-piece), in the breathing circuit, and on the patient and expiratory filters. The percentages of NaF recovered from the nebulizer, breathing circuit, patient filter, and expiratory filter were, respectively, 29.9 ± 8.3, 40.4 ± 5.6, 8.3 ± 1.5, and $21.5 \pm 2.1\%$ (mean $\pm$ standard deviation, n $= 3$) for air, and 32.6 ± 2.2, 36.3 ± 0.7, 12.0 ± 1.4, and $19.1 \pm 1.1\%$ for He/O_2. The increase in the percentage of NaF reaching the patient filter for He/O_2 compared to air was statistically significant ($p < 0.05$). Deposition in the breathing circuit is further subdivided into the Y-piece, flow sensor, and elbow tubing in Figure 9.

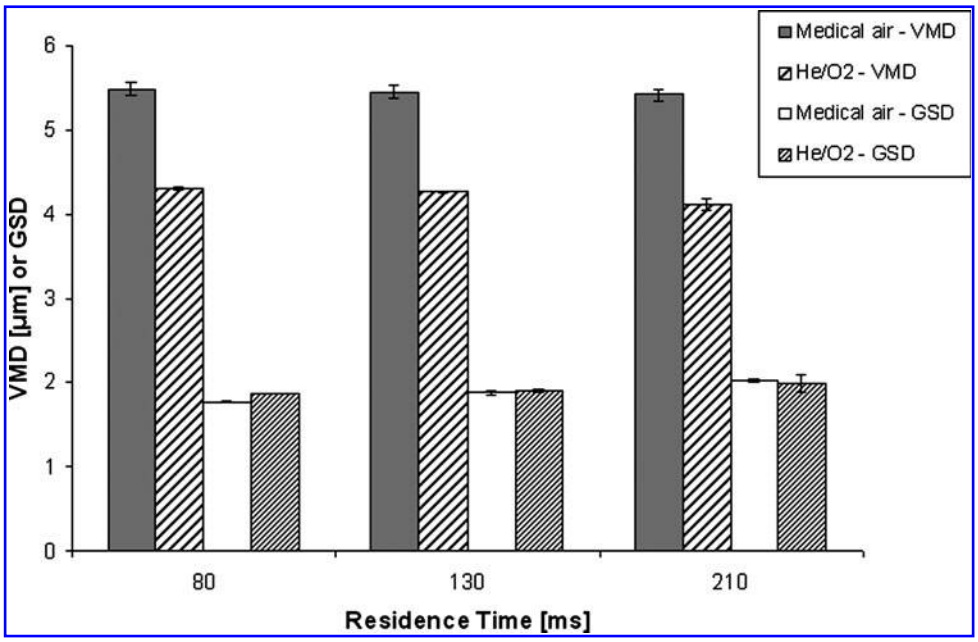

FIG. 7. Volume median diameter (VMD) and geometric standard deviation (GSD) of droplet size distributions measured for the Aeroneb Solo in dry air or He/O_2, with different residence times in tubing between the nebulizer and the laser diffraction measurement chamber. Columns represent the average of three experiments, and error bars represent 1 standard deviation.

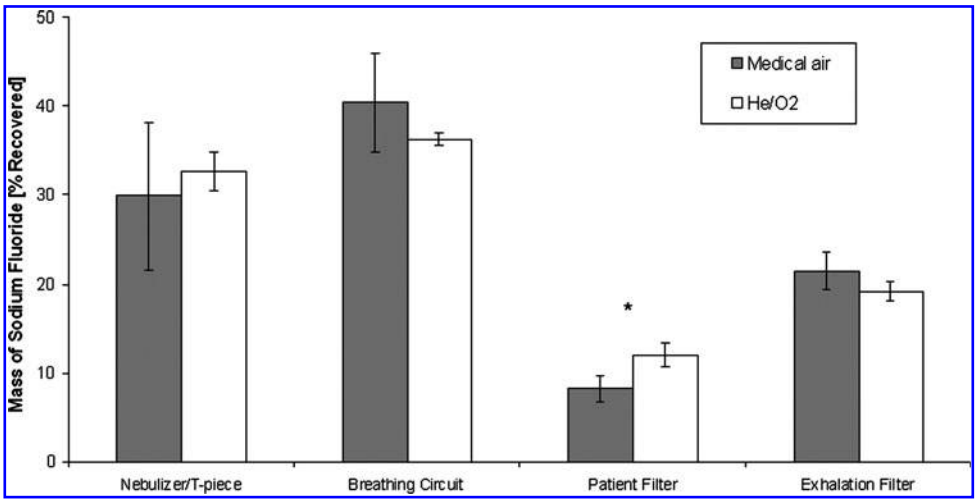

FIG. 8. Deposition of aerosolized sodium fluoride solution in the nebulizer, including T-piece, the breathing circuit, and on the patient and expiratory filters, for ventilation with air or He/O_2. Error bars represent the standard deviation of the data ($n = 3$) around the average value. The asterisk indicates a statistically significant difference ($p < 0.05$).

Discussion

In the present work, droplet size distributions produced by Aeroneb Solo nebulizers were measured using laser diffraction in air and in a mixture containing 78% He and 22% O_2. Droplet sizes were determined for both gases at the exit of the nebulizer T-piece and at the patient end of the breathing circuit of a Hamilton G5 ventilator. Further experiments were performed to determine the effects on measured size distributions of gas humidification and of the droplet residence time during transport from the nebulizer to the laser diffraction measurement volume. Finally, aerosol deposition in the nebulizer, breathing circuit, and on filters placed in the expiratory limb and at the patient end of the breathing circuit, was determined by colorimetry following nebulization of sodium fluoride solutions into the breathing circuit during simulated patient breathing.

Measured droplet sizes exiting the T-piece of Aeroneb Solo nebulizers were smaller in He/O_2 than in air. This result is consistent with the data of O'Callaghan and colleagues,[16] wherein a similar difference was reported between air and He/O_2 for the Aeroneb Pro. In the present work, when the supplied gases were humidified differences in droplet sizes between air and He/O_2 were less pronounced, suggesting that these differences were related to droplet evaporation between nebulization and measurement. As droplet sizes in both air and He/O_2 were unaffected by increased residence time between nebulization and measurement, it appears also that in all cases equilibrium conditions were reached, owing to two-way coupling between droplet evaporation and humidification of the entraining gas,[25,26] prior to measurement. Accordingly, it may be deduced that equilibrium droplet sizes were smaller in He/O_2 than in air, which has been reasoned theoretically due to the difference in the properties of the two gases.[18] More precisely, the product of

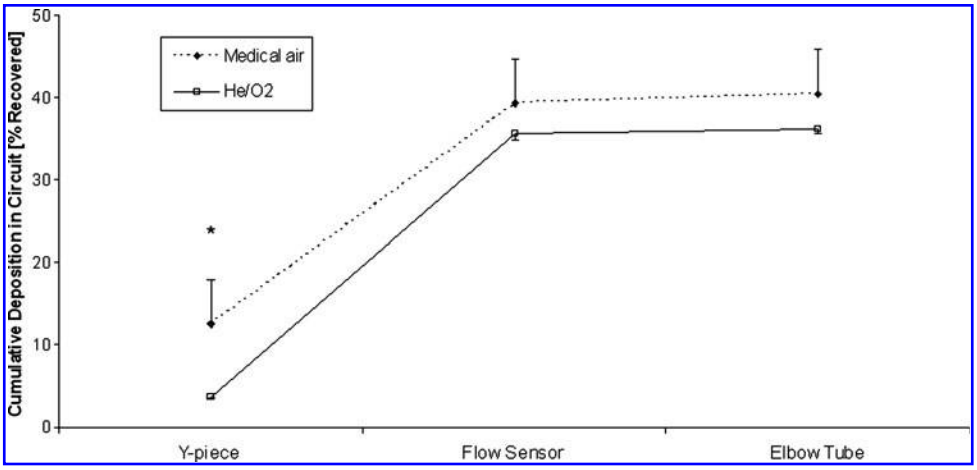

FIG. 9. Cumulative deposition of aerosolized sodium fluoride solution in the three components of the breathing circuit between the nebulizer and patient filter, for ventilation with air or He/O_2. Error bars represent the standard deviation of the data ($n = 3$) around the average value. The asterisk indicates a statistically significant difference ($p < 0.05$).

specific heat capacity and density, which can be thought of as a volume-specific heat capacity, is one of several mechanical and thermal parameters that are different for He/O_2 than for air. If as a result a given volume of He/O_2 cools to a lesser extent than an equivalent volume of air in providing energy for water to transition from the liquid to the vapor phase, more water must evaporate from droplets to saturate He/O_2 than air (because the saturation water vapor concentration in the gas phase decreases with temperature) resulting in smaller droplet sizes at equilibrium.

Droplet sizes were also measured at the patient end of the ventilator breathing circuit, in order to estimate those that, *in vivo*, would pass through the breathing circuit and reach patient facemasks during NIV. Although the 20 L/min flow rate used during size measurements is on the low end of those expected to be delivered during NIV, higher flow rates would have further diluted the aerosol stream, leading to unacceptably low signal-to-noise ratios for laser diffraction measurements made with the breathing circuit in place. For both gases, droplets passing through the breathing circuit were on average considerably smaller than those exiting the nebulizer T-piece. This is no doubt due to size selective deposition losses in the breathing circuit, as reflected in the large deposition fractions measured in the breathing circuit, particularly in the proximal flow sensor. The small reduction in deposition measured in the breathing circuit for He/O_2 compared to air may explain the slightly larger VMD of droplets passing through the circuit with He/O_2 supplied. Certainly, particle Stokes numbers will be somewhat smaller in He/O_2 than in air (the viscosity of He/O_2 78/22 is approximately 20% greater than that of air at 20°C and 1 atm), indicating reduced probabilities of inertial impaction. In addition, inertial impaction in the breathing circuit likely also depends on changes in gas flow patterns with the flow Reynolds number, as is the case for deposition in the mouth–throat.[27] In this context, it is the low density of He/O_2 (approximately one-third that of air, for He/O_2 78/22) that reduces the Reynolds number, and, potentially, deposition in the breathing circuit.

Although aerosol delivery could be altered by changing the position of the nebulizer in the breathing circuit,[11,28,29] the position adopted in the present study is that specified in the ventilator operator's manual, and is thus considered the normal position of use. In addition, the present deposition measurements were made while ventilating with dry gases, whereas previous studies have demonstrated that humidification of ventilator gases can significantly increase aerosol deposition in breathing circuits.[30–35] However, unlike conventional mechanical ventilation, a requirement for humidification during NIV has not been established,[36,37] so that experiments performed with dry gases remain relevant to clinical application. It should also be reiterated that the results presented above are specific to the nebulizer and breathing circuit used in this study. Regarding the latter, the dual limb circuit employed here is typical of intensive care unit (ICU) ventilators, which are widely employed to deliver NIV in critical care settings,[38,39] although practice may very geographically, or from institution to institution. For NIV applied instead using a bilevel ventilator, with a single-limb circuit, the underlying thermophysical effects of He/O_2 on aerosol delivery will be unchanged, but their impact on delivered droplet sizes and aerosol mass would need to be evaluated.

As the main objective of the present work was to evaluate aerosol administration in He/O_2 compared to air using a specific combination of delivery device and ventilator breathing circuit, it is prudent now to estimate how the small differences in droplet size distribution and aerosol delivery through the breathing circuit measured between the two gases might affect delivered lung doses. For this purpose, the equation recently developed by Sandeau et al.[40] may be employed, which predicts deposition in the mouth and throat based on computational results simulating mouth–throat deposition during oral, tidal breathing of air, or He/O_2. For droplet sizes as measured for air and He/O_2 at the patient end of the breathing circuit, and for a breathing pattern identical to that used in the deposition studies, the percentage of inhaled aerosol mass depositing in the mouth and throat is predicted to be just 4.7% for air, and 2.6% for He/O_2. Accordingly, the differences measured between the two gases in aerosol delivery through the breathing circuit are expected to persist into the lung, although it should be noted that in making this prediction potentially larger extrathoracic losses in or around patient facemasks, or during nasal breathing, have been neglected. In particular, leaks at the patient–mask interface are common during NIV,[41] and could have a significant impact on inhaled aerosol mass. Furthermore, given the small sizes of inhaled droplets for both air and He/O_2, it is likely that a substantial fraction of the aerosol entering the lung would be exhaled for both gases; however, the effects of He/O_2 on regional transport and deposition of aerosols in obstructed lungs remains a subject for further study.

In conclusion, ventilation with He/O_2 in place of air led to slightly larger droplet sizes measured at the patient end of a breathing circuit used for NIV, and allowed a greater mass of aerosol to pass through the breathing circuit to reach the patient filter. It should be emphasized that these differences were relatively small, so that their clinical significance would need to be assessed for a particular combination of drug and indication. When incorporating He/O_2 into patient ventilation strategies, assessment of its effects on aerosol delivery is important, so as to distinguish these from the beneficial effects of He/O_2 as a therapy in its own right.

Author Disclosure Statement

A.M., I.K., G.C., and J.T. are current employees of Air Liquide Santé International. A.A. and S.H. are past employees of Air Liquide. Otherwise, no conflicts of interest exist.

References

1. Jolliet P, Tassaux D, Roeseler J, Burdet L, Broccard A, D'Hoore W, Borst F, Reynaert M, Schaller MD, and Chevrolet JC: Helium–oxygen versus air–oxygen noninvasive pressure support in decompensated chronic obstructive disease: a prospective, multicenter study. Crit Care Med. 2003;31:878–884.
2. Maggiore SM, Richard JCM, Abroug F, Diehl JL, Antonelli M, Sauder P, Mancebo J, Ferrer M, Lellouche F, Lecourt L, Beduneau G, and Brochard L: A multicenter, randomized trial of noninvasive ventilation with helium–oxygen mixture in exacerbations of chronic obstructive lung disease. Crit Care Med. 2010;38:145–151.

3. Jaber S, Fodil R, Carlucci A, Boussarsar M, Pigeot J, Lemaire F, Harf A, Lofaso F, Isabey D, and Brochard L: Noninvasive ventilation with helium–oxygen in acute exacerbations of chronic obstructive pulmonary disease. Am J Respir Crit Care Med. 2000;161:1191–1200.
4. Despas PJ, Leroux M, and Macklem PT: Site of airway obstruction in asthma as determined by measuring maximal expiratory flow breathing air and a helium–oxygen mixture. J Clin Invest. 1972;51:3235–3243.
5. Jolliet P, Tassaux D, Thouret JM, and Chevrolet JC: Beneficial effects of helium: oxygen versus air:oxygen noninvasive pressure support in patients with decompensated chronic obstructive pulmonary disease. Crit Care Med. 1999;27:2422–2429.
6. Celli BR, MacNee W, Agusti A, Anzueto A, Berg B, Buist AS, Calverley PMA, Chavannes N, Dillard T, Fahy B, Fein A, Heffner J, Lareau S, Meek P, Martinez F, McNicholas W, Muris J, Austegard E, Pauwels R, Rennard S, Rossi A, Siafakas N, Tiep B, Vestbo J, Wouters E, and ZuWallack R: Standards for the diagnosis and treatment of patients with COPD: a summary of the ATS/ERS position paper. Eur Respir J. 2004;23:932–946.
7. Global Initiative for Chronic Obstructive Lung Disease: *Global Strategy for the Diagnosis, Management and Prevention of Chronic Obstructive Pulmonary Disease*. Medical Communications Resources, Inc., Bethesda, MD; 2009.
8. Maltais F, Ostinelli J, Bourbeau J, Tonnel AB, Acquemet N, Haddon J, Rouleau M, BoukhanA M, Martinot JB, and Duroux P: Comparison of nebulized budesonide and oral prednisolone with placebo in the treatment of acute exacerbations of chronic obstructive pulmonary disease. A randomized controlled trial. Am J Respir Crit Care Med. 2002;165:698–703.
9. Gunen H, Hacievliyagil SS, Yetkin O, Gulbas G, Mutlu LC, and In E: The role of nebulised budesonide in the treatment of exacerbations of COPD. Eur Respir J. 2007;29:660–667.
10. Cazzola M, Noschese P, De Michele F, D'Amato G, and Matera MG: Effect of formoterol/budesonide combination on arterial blood gases in patients with acute exacerbation of COPD. Respir Med. 2006;100:212–217.
11. Calvert LD, Jackson JM, White JA, Barry PW, Kinnear WJ, and O'Callaghan C: Enhanced delivery of nebulised salbutamol during non-invasive ventilation. J Pharm Pharmacol. 2006;58:1553–1557.
12. Mukhopadhyay A, Dela Pena E, Wadden B, Procyshyn M, and Keang Lim T: Effects of inhalational bronchodilator treatment during noninvasive ventilation in severe chronic obstructive pulmonary disease exacerbations. J Crit Care. 2009;24:474.
13. Goode ML, Fink JB, Dhand R, and Tobin MJ: Improvement in aerosol delivery with helium–oxygen mixtures during mechanical ventilation. Am J Respir Crit Care Med. 2001;163:109–114.
14. Corcoran TE, Dauber JH, Chigier N, and Iacono AT: Improving drug delivery from medical nebulizers: the effects of increased nebulizer flow rates and reservoirs. J Aerosol Med. 2002;15:271–282.
15. Piva JP, Menna Barreto SS, Zelmanovitz F, Amantéa S, and Cox P: Heliox versus oxygen for nebulized aerosol therapy in children with lower airway obstruction. Pediatr Crit Care Med. 2002;3:6–10.
16. O'Callaghan C, White J, Jackson J, Crosby D, Dougill B, and Bland H: The effects of heliox on the output and particle-size distribution of salbutamol using jet and vibrating mesh nebulizers. J Aerosol Med. 2007;20:434–444.
17. Hess DR, Acosta FL, Ritz RH, Kacmarek RM, and Camargo CA Jr: The effect of heliox on nebulizer function using a beta-agonist bronchodilator. Chest. 1999;115: 184–189.
18. Martin AR, Gleske J, Katz IM, Hartmann M, Mullinger B, Haussermann S, Caillibotte G, and Scheuch G: Laser diffraction characterization of droplet size distributions produced by vibrating mesh nebulization in air and a helium–oxygen mixture. J Aerosol Sci. 2010;41:1159–1166.
19. Fink JB: Opportunities and risks of using heliox in your clinical practice. Respir Care. 2006;51:651–660.
20. Hess DR: Heliox and noninvasive positive-pressure ventilation: a role for heliox in exacerbations of chronic obstructive pulmonary disease? Respir Care. 2006;51:640–650.
21. Mitchell JP, Nagel MW, Nichols S, and Nerbrink O: Laser diffractometry as a technique for the rapid assessment of aerosol particle size from inhalers. J Aerosol Med. 2006;19: 409–433.
22. Rao N, Kadrichu N, and Ament B: Application of a droplet evaporation model to aerodynamic size measurement of drug aerosols generated by a vibrating mesh nebulizer. J Aerosol Med. 2010;23:295–302.
23. Diaz O, Iglesia R, Ferrer M, Zavala E, Santos C, Wagner PD, Roca J, and Rodriguez-Roisin R: Effects of noninvasive ventilation on pulmonary gas exchange and hemodynamics during acute hypercapnic exacerbations of chronic obstructive pulmonary disease. Am J Respir Crit Care Med. 1997;156:1840–1845.
24. Waldrep JC, Berlinski A, and Dhand R: Comparative analysis of methods to measure aerosols generated by a vibrating mesh nebulizer. J Aerosol Med. 2007;20: 310–319.
25. Finlay WH and Stapleton KW: The effect on regional lung deposition of coupled heat and mass transfer between hygroscopic droplets and their surrounding phase. J Aerosol Sci. 1995;26:655–670.
26. Finlay WH: *The Mechanics of Inhaled Pharmaceutical Aerosols: An Introduction*. Academic Press, London; 2001.
27. Grgic B, Finlay WH, Burnell PKP, and Heenan, AF: In vitro intersubject and intrasubject deposition measurements in realistic mouth–throat geometries. J Aerosol Sci. 2004;35: 1025–1040.
28. Chatmongkolchart S, Schettino GP, Dillman C, Kacmarek RM, and Hess DR: In vitro evaluation of aerosol bronchodilator delivery during noninvasive positive pressure ventilation: effect of ventilator settings and nebulizer position. Crit Care Med. 2002;30:2515–2519.
29. Ari A, Atalay OT, Harwood R, Sheard MM, Aljamhan EA, and Fink JB: Influence of nebulizer type, position, and bias flow on aerosol drug delivery in simulated pediatric and adult lung models during mechanical ventilation. Respir Care. 2010;55:845–851.
30. Ari A, Areabi H, and Fink JB: Evaluation of aerosol generator devices at 3 locations in humidified and non-humidified circuits during adult mechanical ventilation. Respir Care. 2010;55:837–844.
31. Diot P, Morra L, and Smaldone GC: Albuterol delivery in a model of mechanical ventilation: comparison of metered-dose inhaler and nebulizer efficiency. Am J Respir Crit Care Med. 1995;152:1391–1394.
32. Fink JB, Dhand R, Duarte AG, Jenne JW, and obin MJ: Aerosol delivery from a metered-dose inhaler during mechanical ventilation. Am J Respir Crit Care Med. 1996;154: 382–387.

33. Fuller HD, Dolovich MB, Chambers C, and Newhouse MT: Aerosol delivery during mechanical ventilation: a predictive in-vitro lung model. J Aerosol Med. 1992;5:251–259.
34. Martin AR and Finlay WH: The effect of humidity on the size of particles delivered from metered-dose inhalers. Aerosol Sci Technol. 2005;39:283–289.
35. O'Riordan TG, Greco MJ, Perry RJ, and Smaldone GC: Nebulizer function during mechanical ventilation. Am Rev Respir Dis. 1992;145:1117–1122.
36. Branson RD and Gentile MA: Is humidification always necessary during noninvasive ventilation in the hospital? Respir Care. 2010;55:209–216.
37. Ricard J-D and Boyer A: Humidification during oxygen therapy and non-invasive ventilation: do we need some and how much? Intensive Care Med. 2009;35:963–965.
38. Demoule A, Girou E, Richard JC, Taille S, and Brochard L: Increased use of noninvasive ventilation in French intensive care units. Intensive Care Med. 2006;32:1747–1755.
39. Vignaux L, Tassaux D, Carteaux G, Roeseler J, Piquilloud L, Brochard L, and Jolliet P: Performance of noninvasive ventilation algorithms on ICU ventilators during pressure support: a clinical study. Intensive Care Med. 2010;36:2053–2059.
40. Sandeau J, Katz I, Fodil R, Louis B, Apiou-Sbirlea G, Caillibotte G, and Isabey D: CFD simulation of particle deposition in a reconstructed human oral extrathoracic airway for air and helium–oxygen mixtures. J Aerosol Sci. 2010;41: 281–294.
41. Vignaux L, Vargas F, Roeseler J, Tassaux D, Thille AW, Kossowsky MP, Brochard L, and Jolliet P: Patient–ventilator asynchrony during noninvasive ventilation for acute respiratory failure: a multicenter study. Intensive Care Med. 2009;35:840–846.

Received on December 3, 2010
in final form, February 17, 2011

Reviewed by:
Timothy Corcoran
Dean Hess

Address correspondence to:
Andrew R. Martin, Ph.D.
Medical Gases Group
Air Liquide Santé International
Centre de Recherche Claude-Delorme
1 chemin de la Porte des Loges, Les Loges-en-Josas
BP 126-78354 Jouy-en-Josas, Cedex France

E-mail: andrew-r.martin@airliquide.com